

Joint spatial–directional localization features of wave fields focused at a complex point

Miguel A. Alonso

The Institute of Optics, University of Rochester, Rochester, New York 14627

Riccardo Borghi

Istituto Nazionale per la Fisica della Materia, Dipartimento di Elettronica Applicata, Università Roma Tre Via della Vasca Navale, 84 I-00146 Rome, Italy

Massimo Santarsiero

Istituto Nazionale per la Fisica della Materia, Dipartimento di Fisica, Università Roma Tre Via della Vasca Navale, 84 I-00146 Rome, Italy

Received June 2, 2005; revised September 2, 2005; accepted September 16, 2005; posted September 23, 2005 (Doc. ID 62528)

A systematic study of the joint spatial–directional localization features of monochromatic wave fields focused at a complex point is presented, on the basis of recently introduced measures of spatial and directional spread for wide-angle wave fields. Such features are compared with those of a class of fields defined to achieve the theoretical minimum product of these spread measures. It is found that the two classes of fields are remarkably similar. © 2006 Optical Society of America

OCIS codes: 350.5500, 260.2110.

1. INTRODUCTION

In Refs. 1 and 2 we found the lower bounds for the spatial and directional spread measures, as defined in Ref. 3, for free nonparaxial monochromatic scalar and vector fields. These lower bounds are achieved by families of fields, referred to as minimum uncertainty fields (MUFs), which were obtained as eigenfunctions of a differential operator found through a variational approach. These fields do not have a simple closed-form expression, and must be computed through a multipolar expansion.

The MUFs constitute a generalization of Gaussian beams into the nonparaxial regime. It is interesting to recall, however, that there are other such generalizations. A particularly elegant option corresponds to fields generated by point sources at a complex location. The connection between these fields and Gaussian beams was first noticed by Kravtsov,⁴ Arnaud,⁵ Keller and Streifer,⁶ and Deschamps.⁷ These fields have been extensively studied by Felsen and collaborators.^{8–11} In our context, however, it is more convenient to consider instead spherical waves focused at a complex point (which can be thought of as the superposition of a coincident source–sink pair). This modification removes the singular behavior found in this type of fields.^{10,12,13} The vectorial analogs of these fields were first proposed by Cullen and Yu,¹⁴ and studied extensively by Sheppard and Saghafi.^{15–17}

Both the MUFs and the complex focus fields (CFFs) give a continuous transition between a Gaussian beam and a perfectly focused spherical wave. However, unlike for the MUFs, the angular spectrum for the CFFs is given by a remarkably simple expression, and the corresponding measures of spread can be calculated in closed form. It

will be shown here that these fields are indeed surprisingly good approximations to the MUFs.

2. MINIMUM UNCERTAINTY FIELDS

A. Scalar Case

A scalar free field can be expanded in terms of plane waves in the form

$$U(\mathbf{r}) = \int_{4\pi} A(\mathbf{u}) \exp(i\mathbf{u} \cdot \mathbf{r}) d\Omega, \quad (1)$$

where \mathbf{u} is a unit vector, $A(\mathbf{u})$ is the angular spectrum of the field, and the position vector \mathbf{r} is in units of reduced wavelengths. For paraxial fields, A is significantly different from zero only for \mathbf{u} within a small solid angle around a specific direction, usually associated with that of the positive z axis. For nonparaxial fields, A can take any value for any \mathbf{u} (even when the z component of \mathbf{u} is negative). In this case, the usual measures of spatial and directional spread are no longer appropriate. For this reason, suitable measures of spread for nonparaxial fields were proposed in Ref. 3. If we choose the main direction of propagation to be aligned with the z axis, the measure of directional spread is given by the expression

$$\Delta_\theta = \arccos \left[\frac{\int_{4\pi} |A(\mathbf{u})|^2 \cos \theta d\Omega}{\int_{4\pi} |A(\mathbf{u})|^2 d\Omega} \right], \quad (2)$$

where θ is the polar angle (that is, $\cos \theta = u_z$). The ratio of the integrals in the argument of the arccosine has a

simple interpretation: It is the distance from the origin to the centroid of a spherical shell of unit radius centered at the origin and with surface mass density proportional to $|A(\mathbf{u})|^2$. Therefore Δ_θ corresponds to the half-angle of the cone whose vertex is the origin and that contains the circle corresponding to the intersection of the unit sphere and a plane containing the centroid with normal in the z direction (see Fig. 1 of Ref. 1). The measure of spatial spread, on the other hand, is given by

$$\Delta_r = \left[\frac{\int_{4\pi} A^*(\mathbf{u})L^2A(\mathbf{u})d\Omega}{\int_{4\pi} |A(\mathbf{u})|^2d\Omega} \right]^{1/2}, \tag{3}$$

where L^2 is the square of the angular-momentum operator, defined by

$$L^2 = -\frac{1}{\sin\theta} \frac{\partial}{\partial\theta} \left[\sin\theta \frac{\partial}{\partial\theta} \right] - \frac{1}{\sin^2\theta} \frac{\partial^2}{\partial\phi^2}, \tag{4}$$

with ϕ being the azimuthal angle. It is assumed here that the origin is placed at the centroid of the field, i.e., at the point where the measure in Eq. (3) is minimal. Physical interpretations for this measure are given in Refs. 1 and 3.

In Ref. 1 we searched for the fundamental lower bounds of these measures of spread. Such lower bounds are the extension into the nonparaxial regime of the well-known uncertainty relation. They are achieved by a family of fields, referred to as MUFs, which are a nonparaxial extension of Gaussian beams. It was found through a variational treatment that the angular spectra of these fields are the ground-state (i.e., lowest eigenvalue) eigenfunctions of a second-order operator of the form

$$\mathcal{Q}_s = \frac{2}{w^4}(1 - \cos\theta) + L^2, \tag{5}$$

where the subscript s stands for scalar and w is a parameter that regulates the angular spread of the MUF.

Unlike for the case of two-dimensional (2D) MUFs, for which eigenfunctions of the operator in Eq. (5) can be expressed in terms of standard functions, the angular spectra of the three-dimensional (3D) MUFs must be found numerically. This was done in Ref. 1 through a decomposition into spherical harmonics. In particular, it was found that scalar MUFs give a continuous transition between spherical waves (for $w \rightarrow \infty$) and paraxial Gaussian beams (for $w \rightarrow 0$).

B. Vectorial Case

Analogous lower bounds apply for vector fields. Let us consider the electric field \mathbf{E} of a monochromatic electromagnetic wave in free space. The angular spectrum of this field must now be a vector, i.e.,

$$\mathbf{E}(\mathbf{r}) = \int_{4\pi} \mathbf{A}(\mathbf{u})\exp(i\mathbf{u} \cdot \mathbf{r})d\Omega, \tag{6}$$

where the transversality condition requires that $\mathbf{A}(\mathbf{u}) \cdot \mathbf{u} = 0$. The measures of spread are defined in analogous forms:

$$\Delta_\theta = \arccos \left[\frac{\int_{4\pi} |\mathbf{A}(\mathbf{u})|^2 \cos\theta d\Omega}{\int_{4\pi} |\mathbf{A}(\mathbf{u})|^2 d\Omega} \right], \tag{7}$$

$$\Delta_r = \left[\frac{\int_{4\pi} \mathbf{A}^*(\mathbf{u}) \cdot L^2 \mathbf{A}(\mathbf{u}) d\Omega}{\int_{4\pi} |\mathbf{A}(\mathbf{u})|^2 d\Omega} \right]^{1/2}. \tag{8}$$

By using again a variational approach, it was found in Ref. 2 that the angular spectra of the vectorial MUFs are also the ground-state eigenfunctions of a very similar operator:

$$\mathcal{Q}_v = \frac{2}{w^4}(1 - \cos\theta) + \mathcal{P}_\mathbf{u}L^2, \tag{9}$$

where v now stands for vectorial, and $\mathcal{P}_\mathbf{u}$ is the projection matrix to the plane perpendicular to \mathbf{u} , i.e., $\mathcal{P}_\mathbf{u}\mathbf{C} = \mathbf{C} - (\mathbf{C} \cdot \mathbf{u})\mathbf{u} = \mathbf{u} \times (\mathbf{C} \times \mathbf{u})$. By using an expansion in vector spherical harmonics, the eigenfunctions of this operator were found to have the following general form²:

$$\mathbf{A}_w(\mathbf{u}) = [\alpha\mathbf{U}_1(\mathbf{u}) + \beta\mathbf{U}_2(\mathbf{u})]F_w(\theta), \tag{10}$$

where α and β are constant coefficients, and $F_w(\theta)$ is a scalar function that is found through the series expansion. It turns out that $F_w(\theta)$ becomes 1 for $w \rightarrow \infty$ and tends to be proportional to $\exp[-\theta^2/(2w^2)]$ for small values of w . Furthermore, vectors \mathbf{U}_1 and \mathbf{U}_2 are defined as²

$$\mathbf{U}_1(\mathbf{u}) = (1 + \cos\theta)(\cos\phi\mathbf{e}_\theta - \sin\phi\mathbf{e}_\phi), \tag{11}$$

$$\mathbf{U}_2(\mathbf{u}) = (1 + \cos\theta)(\sin\phi\mathbf{e}_\theta + \cos\phi\mathbf{e}_\phi), \tag{12}$$

where \mathbf{e}_θ , \mathbf{e}_ϕ are unit vectors in the directions of increase of the polar angle θ and the azimuthal angle ϕ , respectively. Notice that \mathbf{U}_1 corresponds to the angular spectrum of the sum of an electric dipole field in the x direction and a magnetic dipole field in the y direction, both with equal amplitudes and phases. Similarly, \mathbf{U}_2 corresponds to the angular spectrum of the sum, with equal amplitudes and phases, of an electric dipole field in the y direction and a magnetic dipole field in the $-x$ direction. These combinations of crossed dipoles are known to achieve maximum focal intensity.^{18,19} The vector MUFs then give a continuous transition between a superposition of dipolar fields (for $w \rightarrow \infty$) and a paraxial Gaussian beam with arbitrary uniform polarization (for $w \rightarrow 0$).

3. FIELDS FOCUSED AT COMPLEX POINTS

A. Scalar Case

A spatial shift in a field $U(\mathbf{r})$ results from replacing \mathbf{r} with $\mathbf{r}-\mathbf{r}_0$, where \mathbf{r}_0 is the point to which the initial origin is translated. Notice from Eq. (1) that this shift is equivalent to a transformation of the angular spectrum according to

$$A(\mathbf{u}) \rightarrow A(\mathbf{u})\exp(-i\mathbf{u} \cdot \mathbf{r}_0). \quad (13)$$

This property is equivalent to the well-known shift-phase property in Fourier analysis.

In particular, since the angular spectrum of a perfect spherical wave focused at the origin is constant, the expression for the angular spectrum of a perfect spherical wave focused at a point \mathbf{r}_0 is given by $A_0 \exp(-i\mathbf{r}_0 \cdot \mathbf{u})$, where A_0 is a constant. Let us now consider placing the focus at the imaginary coordinate $\mathbf{r}_0=iq\mathbf{e}_z$, where $q \geq 0$ and \mathbf{e}_z is the unit vector in the z direction. Then the angular spectrum, say A_q , becomes

$$A_q(\mathbf{u}) = A_0 \exp(qu_z) = A_0 \exp(q \cos \theta). \quad (14)$$

It is easy to see that the spherical symmetry is broken, and that the main direction of propagation corresponds to the z direction, i.e., to the direction of the imaginary part of the position of the focus. The field is largest at the origin, i.e., at the real part of the position of the focus. Observe also that, as q becomes larger, the angular spectrum becomes more sharply peaked, so that the beam is more directional and less spatially localized. In fact, as can be easily verified, for $q \gg 1$ the resulting field becomes a paraxial Gaussian beam having a waist size equal to $\sqrt{2q}$. For smaller q , these fields are nonparaxial generalizations of a Gaussian beam; and as q tends to zero, these fields become completely delocalized directionally, reducing to perfect spherical focused waves for $q=0$. Therefore one expects these fields, referred to in what follows as CFFs, to exhibit a behavior similar to that of the MUFs.

The measures of directional and spatial spread in Eqs. (2) and (3) can be easily calculated in closed form for these fields:

$$\Delta_\theta = \arccos \left[\frac{2q \cosh(2q) - \sinh(2q)}{2q \sinh(2q)} \right], \quad (15)$$

$$\Delta_r = \left[\frac{2q \cosh(2q) - \sinh(2q)}{2 \sinh(2q)} \right]^{1/2}. \quad (16)$$

Notice that $\Delta_r^2 / \cos \Delta_\theta = q$. Figure 1(a) shows the curve $\delta_r = \arctan \Delta_r$ versus Δ_θ for the MUFs (solid curve) and for the CFFs (circles) in the scalar case. Surprisingly, the two curves are practically undistinguishable.

B. Vectorial Case

As stated in Subsection 2.B, in the limit when the spatial localization reaches its fundamental minimum, i.e., for $w \rightarrow \infty$, the MUFs become a sum of electric and magnetic dipole fields, with an angular spectrum given by

$$\mathbf{A}_\infty(\mathbf{u}) = \alpha \mathbf{U}_1(\mathbf{u}) + \beta \mathbf{U}_2(\mathbf{u}). \quad (17)$$

As in the scalar case, we consider moving the focal point of the dipolar fields to the imaginary point $\mathbf{r}_0=iq\mathbf{e}_z$. The

angular spectrum again acquires the usual exponential factor, leading to

$$\mathbf{A}_q(\mathbf{u}) = \exp(q \cos \theta) \mathbf{A}_\infty(\mathbf{u}) = \exp(q \cos \theta) [\alpha \mathbf{U}_1(\mathbf{u}) + \beta \mathbf{U}_2(\mathbf{u})]. \quad (18)$$

Such an angular spectrum defines what we call a vector CFF. The corresponding spatial and directional spread measures follow from the substitution of Eq. (18) into Eqs. (7) and (8). These spreads can also be expressed in closed-form terms:

$$\Delta_\theta = \arccos \left\{ \frac{(-3 + 10q - 16q^2 + 16q^3) \exp(4q) + 3 + 2q}{2q[(1 - 4q + 8q^2) \exp(4q) - 1]} \right\}, \quad (19)$$

$$\Delta_r = \left[\frac{1 + 3q + (-1 + q + 4q^2 + 8q^3) \exp(4q)}{(1 - 4q + 8q^2) \exp(4q) - 1} \right]^{1/2}. \quad (20)$$

Unlike for the scalar case, there is no simple closed-form expression for q in terms of the spreads of vector fields. However, it turns out that these spreads again trace a curve that is practically identical to that pertinent to vectorial MUFs, as one can see in Fig. 1(b).

C. Correspondence between Minimum Uncertainty Fields and Complex Focus Fields

The results obtained so far suggest that there should be a tight correspondence between MUFs and CFFs. Indeed, from Fig. 1 one could even suspect that CFFs are just the

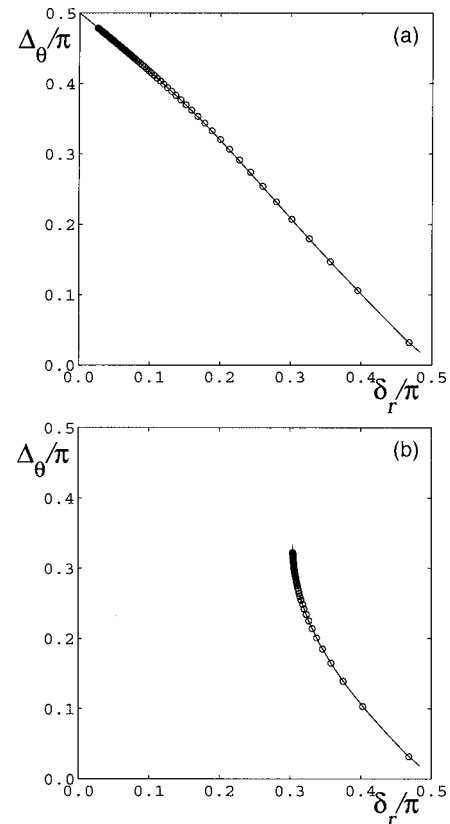


Fig. 1. Behavior of $\delta_r = \arctan \Delta_r$ versus Δ_θ for the MUFs (solid curve) and for the CFFs (circles) in the (a) scalar and (b) vectorial case.

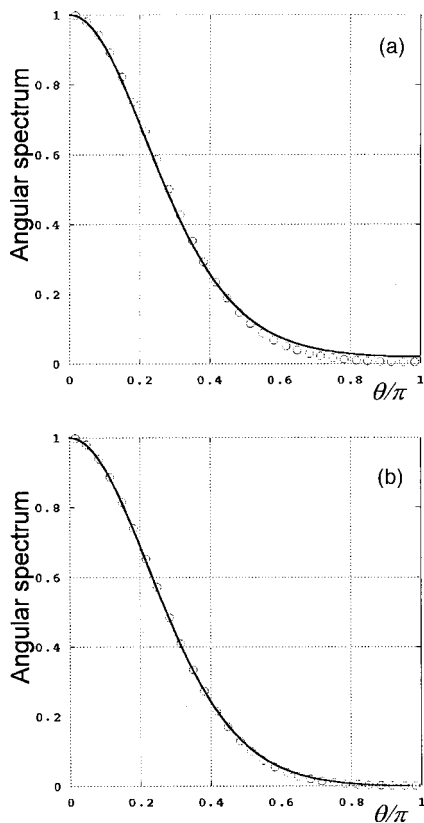


Fig. 2. Behavior of the normalized angular spectrum (circles) of (a) scalar and (b) vectorial MUFs, as functions of θ/π , for $w = 0.7$. Solid curves are best fits obtained by use of Eq. (21) for the scalar case (with $q \approx 1.96$), and Eq. (22) for the vectorial case (with $q \approx 1.43$).

MUFs found in Refs. 1 and 2. This is not the case, however, as shown by the comparison of their angular spectra in Fig. 2. In particular, we have considered scalar and vectorial MUFs having $w = 0.7$, whose normalized angular spectra are plotted (circles) as functions of θ/π . The solid curves represent a best fit obtained with the functions

$$A(\theta) = \exp[q(\cos \theta - 1)], \tag{21}$$

for the scalar case and

$$A(\theta) = \frac{1 + \cos \theta}{2} \exp[q(\cos \theta - 1)] \tag{22}$$

for the vectorial case.

Figure 2 shows that the CFFs are very similar but not identical to the MUFs. Moreover, from Fig. 1 we realize that there is an approximate one-to-one correspondence between these fields. To describe such correspondence in quantitative terms, in Fig. 3 the values of q obtained as in Fig. 2 are reported for several values of w (circles), both in the scalar and vectorial cases. In particular, it can be seen that, for small values of w (i.e., for $w < 1$), one has $q \approx 1/w^2$ in both cases. In the opposite limit (i.e., for $w > 1$), instead, the relationship $w \rightarrow q$ depends on the nature of the fields. For scalar fields one finds $q \approx 1/w^4$, while in the vectorial case $q \approx 1/2w^4$. This different asymptotic behavior between scalar and vector fields will be explained in Section 4.

So far we have only shown that the CFFs are not exact MUFs for the pair Δ_r, Δ_θ defined in Refs. 1 and 2. But why are they so close to the MUFs? In Section 4 we give an explanation of this notable similarity. What we will find is that the CFFs are themselves MUFs, but for different definitions of the angular spread measure.

4. COMPLEX FOCUS FIELDS AS MINIMUM UNCERTAINTY FIELDS

A. Lower Bounds and Commuting Relations

Within the context of quantum optics, it is well known that functions of the type $\exp(q \cos \theta)$ define a class of minimum uncertainty states for certain measures of spread of the photon number and phase (see, for instance, Ref. 20). We now take advantage of the mathematical analogy between the quantum number-phase problem and the case of 2D classical scalar fields for establishing a link with the MUFs proposed in Refs. 1 and 2. The subsequent step consists on generalizing this analogy to the 3D scalar and vectorial cases. We will show that it is possible to find suitable angular spread measures for which the CFFs indeed constitute MUFs. What is more important is the fact that these measures, whose definitions are considerably different from the one for Δ_θ , lead to remarkably similar values for the angular spread of the CFFs. This, in turn, explains why MUFs and CFFs are practi-

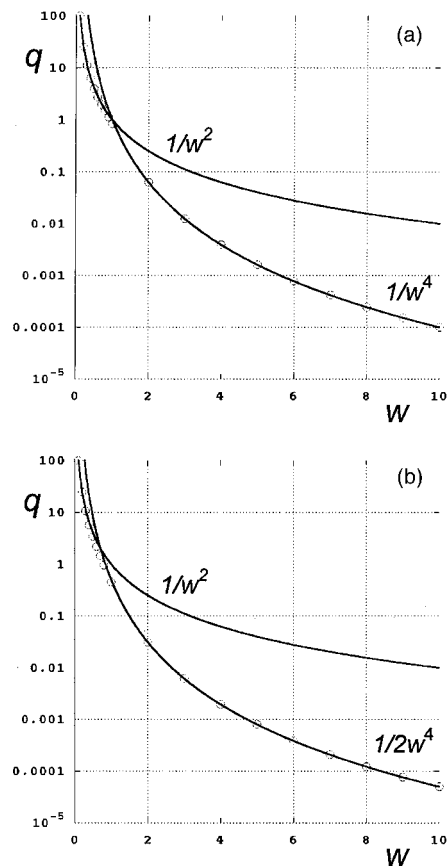


Fig. 3. Correspondence between the parameters q (corresponding to the CFFs) and w (corresponding to the MUFs) provided by a best fit of the corresponding angular spectra for (a) scalar and (b) vector fields. The solid curves indicate the asymptotic behaviors.

cally undistinguishable: They minimize measures that are very similar. For the scalar case, the corresponding new measure of angular spread is tied to the measure of spatial spread proposed earlier through a simple uncertainty relation.

We start by deriving the uncertainty relation in the 2D scalar case by noting that the direction vector is now given by $\mathbf{u} \equiv (u_x, u_z) = (\sin \theta, \cos \theta)$, where $\theta \in [0, 2\pi)$ and the angular-momentum operator is a scalar, given by $L = -i\partial/\partial\theta$. Furthermore, recall that z was chosen as the main direction of propagation of the field, so u_x is then the transverse component of the wave vector. Its commutator with the angular-momentum operator is given by

$$[u_x, L] = iu_z. \quad (23)$$

By using the standard procedure based on the Cauchy–Schwarz inequality, one obtains the relation

$$\Delta_L^2 \Delta_{u_x}^2 \geq \frac{\langle u_z^2 \rangle}{4} + \frac{\langle \{u_z, L\} \rangle^2}{4} \geq \frac{\langle u_z^2 \rangle}{4}, \quad (24)$$

where the braces denote the anticommutator and, for any operator \mathcal{O} ,

$$\Delta_{\mathcal{O}}^2 = \langle \mathcal{O}^2 \rangle - \langle \mathcal{O} \rangle^2, \quad (25)$$

$$\langle \mathcal{O} \rangle = \frac{\int_{2\pi} A^*(\mathbf{u}) \mathcal{O} A(\mathbf{u}) d\theta}{\int_{2\pi} |A(\mathbf{u})|^2 d\theta}. \quad (26)$$

Since $\Delta_L = \Delta_r$ and $\langle u_x \rangle = 0$ (due to the appropriate choices of the origin and the z axis), the relation in Eq. (24) can be written, after simple algebra, as

$$\Delta_r \tan \tilde{\Delta}_\theta \geq \frac{1}{2}, \quad (27)$$

where a different directional spread measure, namely, $\tilde{\Delta}_\theta$, which is an alternative to Δ_θ , is defined as

$$\tilde{\Delta}_\theta = \arctan\left(\frac{\Delta_{u_x}}{\langle u_z \rangle}\right) = \arctan\left(\frac{\sqrt{\langle \sin^2 \theta \rangle}}{\langle \cos \theta \rangle}\right). \quad (28)$$

It must be stressed, however, that unlike the measure Δ_θ , the new measure $\tilde{\Delta}_\theta$ does not have a simple geometric interpretation in terms of the centroid of the unit ring weighted by the angular spectrum.^{21,22}

Notice that inequality Eq. (27) is very similar to the one given in Ref. 1 involving the measure of directional spread Δ_θ . However, unlike that relation, the one in inequality (27) can be satisfied as an equality. In fact, as is well known from the usual derivation of the Cauchy–Schwarz inequality, the first relation in inequality (24) is satisfied as an equality for angular spectra when $LA(\mathbf{u})$ is proportional to $u_x A(\mathbf{u})$. This is indeed the case for the CFFs, since it is straightforward to prove that

$$LA_q(\mathbf{u}) = iqu_x A_q(\mathbf{u}). \quad (29)$$

Additionally, since A_q is real, the anticommutator term that was dropped in inequality (24) is easily shown to

vanish, so both relations in this equation become equalities, as does inequality (27).

To extend the above results to 3D scalar fields, we first notice that for the angular spectrum of the CFFs,

$$\mathbf{L}A_q(\mathbf{u}) = iq\mathbf{e}_z \times \mathbf{u}A_q(\mathbf{u}). \quad (30)$$

Therefore we consider the uncertainty relation given by

$$\Delta_{\mathbf{L}}^2 \Delta_{\mathbf{e}_z \times \mathbf{u}}^2 \geq \frac{\langle [L_j, \{\mathbf{e}_z \times \mathbf{u}\}_j] \rangle^2}{4}, \quad (31)$$

where the convention of implicit sum over repeated indices is used, and the anticommutator term was dropped. [Because Eq. (30) and the fact that A_q is real, we know from the outset that the angular spectrum of the CFFs makes inequality (31) be satisfied as an equality.] Again, we can replace $\Delta_{\mathbf{L}}^2 = \Delta_r^2$. Similarly, by using the fact that $\langle u_x \rangle = \langle u_y \rangle = 0$, we can see that $\Delta_{\mathbf{e}_z \times \mathbf{u}}^2 = \langle u_y^2 + u_x^2 \rangle = \langle \sin^2 \theta \rangle$. Finally, from the well-known commutation relation

$$[L_j, u_k] = i\epsilon_{jkm} u_m, \quad (32)$$

where ϵ_{ijk} is the Levi-Civita tensor, one finds that

$$[L_j, \{\mathbf{e}_z \times \mathbf{u}\}_j] = \epsilon_{jzk} [L_j, u_k] = i\epsilon_{jzk} \epsilon_{jkm} u_m = -2iu_z. \quad (33)$$

Therefore, inequality (31) becomes

$$\Delta_r^2 \langle \sin^2 \theta \rangle \geq \langle u_z \rangle^2 = \langle \cos \theta \rangle^2. \quad (34)$$

By using straightforward algebra, we find

$$\Delta_r \tan \tilde{\Delta}_\theta \geq 1, \quad (35)$$

where $\tilde{\Delta}_\theta$ is defined by the last expression in Eq. (28). Inequality (35) is thus the 3D counterpart of inequality (27).

The closed-form expression of $\tilde{\Delta}_\theta$ associated with a 3D CFF turns out to be

$$\tilde{\Delta}_\theta = \arctan \sqrt{\frac{2 \sinh(2q)}{2q \cosh(2q) - \sinh(2q)}}. \quad (36)$$

Again, we corroborate from the substitution of Eqs. (16) and (36) into inequality (35) that the CFFs are the MUFs corresponding to the alternative measure of angular spread. Figure 4(a) shows a quantitative comparison between both measures of angular spread for the CFFs as functions of q . We can see that, for these fields, both measures give very similar results (the maximum relative difference being of 7%, corresponding to $q=1.1$). The similarity of these measures for scalar fields like the CFFs clarifies why they are a good approximation of scalar MUFs.

As far as the vectorial case is concerned, there is no simple first-order equation analogous to Eq. (30). This fact should suggest that, differently from the scalar case, vectorial CFFs are not MUFs for the pair $(\Delta_r, \tilde{\Delta}_\theta)$. Nevertheless, it is still possible to express in closed form the angular spread $\tilde{\Delta}_\theta$ pertinent to vectorial CFFs. Figure 4(b) shows the comparison between the two angular measures, in the same way as shown in Fig. 4(a) for the scalar one. We see that even in this case the maximum relative difference between Δ_θ and $\tilde{\Delta}_\theta$ is of 5%, corresponding to $q=0.5$ (which is even better than in the scalar case). That

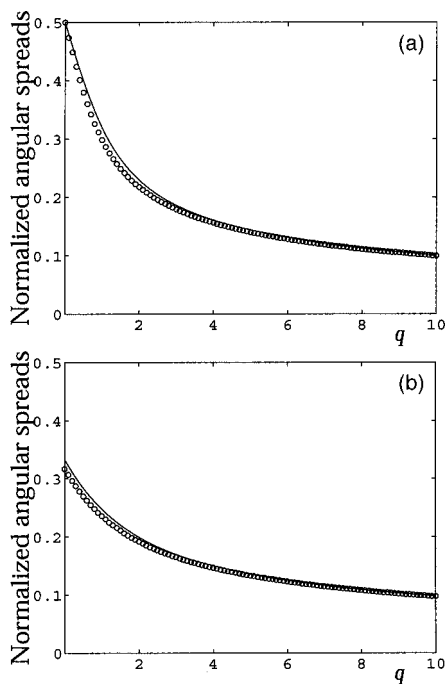


Fig. 4. Behavior, as a function of q , of Δ_θ (solid curve) and $\tilde{\Delta}_\theta$ (circles) in the (a) scalar and (b) vectorial case.

vectorial CFFs are not minimum uncertainty states for the angular measure $\tilde{\Delta}_\theta$ can be rigorously proved by resorting to a variational approach, like was done in Refs. 1 and 2.

B. Variational Approach

By performing a variational procedure analogous to the one presented in Ref. 1, one finds that the angular spectra of scalar fields that jointly minimize Δ_r and $\tilde{\Delta}_\theta$ are eigenfunctions of the operator

$$\mathcal{R}_s = 2q(1 - \cos \theta) + q^2 \sin^2 \theta + L^2, \tag{37}$$

where again s stands for scalar. One can easily verify that Eq. (14) is an eigenfunction of Eq. (37) with an eigenvalue equal to $2q$.²³

Moreover, the direct comparison of the operator \mathcal{R}_s and the operator \mathcal{Q}_s given in Eq. (5) explains the asymptotic behavior shown in Fig. 3(a) as far as the relation $w \leftrightarrow q$ is concerned. In fact, in the limit of small q , the term proportional to q^2 in Eq. (37) can be neglected, and this operator becomes equivalent to the one in Eq. (5), with $q \approx 1/w^4$. In the opposite limit, when q is very large, the term proportional to q^2 in Eq. (37) dominates over the one proportional to q , and \mathcal{R}_s appears to be different from \mathcal{Q}_s . However, in this limit, the angular spectrum is strongly localized within small values of θ . Therefore the cosine in Eq. (5) and the cosine and squared sine in Eq. (37) can be expanded quadratically around $\theta=0$ (valid for small w). By matching the quadratic terms in both operators, it is found that their solutions are similar if $q \approx 1/w^2$. It turns out that, even between these two limiting situations, the two operators can be made to remain similar over the ranges in θ where their ground-state eigenfunctions are significant by choosing the appropriate correspondence between w and q .

On performing the same variational analysis for the vectorial case, and on taking into account that the projection operator \mathcal{P}_u acts only on the spatial measure Δ_r , one obtains that, for vectorial CFFs to be MUFs of the pair Δ_r , $\tilde{\Delta}_\theta$, it is necessary that their angular spectra are eigenfunctions of the operator

$$\mathcal{R}_v = 2q(1 - \cos \theta) + q^2 \sin^2 \theta + \mathcal{P}_u L^2, \tag{38}$$

where v now stands for vector. However, one can show that the angular spectrum of the vector CFFs, given in Eq. (18), is not an eigenfunction of this operator. The angular spectrum of these fields is instead the ground-state eigenfunction of the operator

$$\mathcal{R}'_v = 4q(1 - \cos \theta) + q^2 \sin^2 \theta + \mathcal{P}_u L^2, \tag{39}$$

with the eigenvalue given by $2(q+1)$. Notice the factor of 4, instead of 2, in front of the term proportional to q . This factor explains why the asymptotic behavior for large w shown in Fig. 3(b) is different from that for the scalar case, shown in Fig. 3(a). Also, because of this different factor, for this operator to be the result of a variational derivation, a measure of angular spread must be used that is a monotonic function of the combination $\langle \sin^2 \theta \rangle / \langle \cos \theta \rangle^4$. Because we want to compare this new measure with the ones used earlier, it must be chosen to have units of radians and to be constrained to the interval $[0, \pi/2]$. It is then reasonable to define the measure, denoted by $\hat{\Delta}_\theta$, as the solution of

$$\frac{\sin^2 \hat{\Delta}_\theta}{\cos^4 \hat{\Delta}_\theta} = \frac{\langle \sin^2 \theta \rangle}{\langle \cos \theta \rangle^4}, \tag{40}$$

which, after simple algebra, leads to

$$\hat{\Delta}_\theta = \arccos \left(\sqrt{\frac{2}{1 + \sqrt{1 + 4 \frac{\langle \sin^2 \theta \rangle}{\langle \cos \theta \rangle^4}}}} \right). \tag{41}$$

Apart from the difficulty of giving a physical meaning to such a measure, what we want to point out is that all three different angular spread measures give very similar values for the angular spread of the vector CFFs as shown

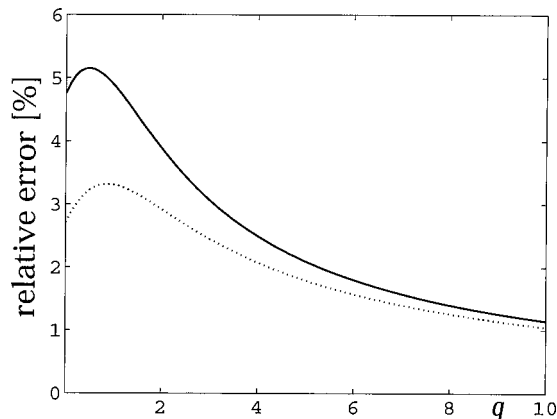


Fig. 5. Behavior, as a function of q , of the relative difference (expressed in percent) between Δ_θ and $\tilde{\Delta}_\theta$ (solid curve) and between Δ_θ and $\hat{\Delta}_\theta$ (dotted curve).

in Fig. 5, where the relative differences (expressed in percent) $|1 - \tilde{\Delta}_\theta/\Delta_\theta|$ and $|1 - \hat{\Delta}_\theta/\Delta_\theta|$ are plotted as solid and dotted curves, respectively.

5. CONCLUSIONS

In the present paper the joint spatial–directional localization features of complex-source fields have been studied in comparison with a recently introduced nonparaxial extension of the fundamental Gaussian beams.^{1,2} In particular, we found that, despite the simple analytical structure of their angular spectra, CFFs provide a class of nonparaxial fields that are surprisingly good approximations to the MUFs and therefore share their optimum joint spatial–directional localization properties.

Vectorial CFFs correspond to combinations of dipolar fields, where the direction of the dipoles is perpendicular to the direction of the imaginary part of their position. Sheppard and Saghafi¹⁷ also studied the case of dipoles aligned with their imaginary displacement. By doing a study like the one presented here, one can easily show that these fields are again similar to the vector fields with minimum uncertainty and azimuthal momentum equal to zero, studied in Ref. 2.

We provided an explanation for the above similarities by showing that CFFs are indeed MUFs, but, corresponding to different angular spread measures, the definitions are different from the one used to obtain the MUFs. The fact that functions of the type $\exp(q \cos \theta)$ are functions with minimum uncertainty was already known within the context of the quantum number-phase problem. Here we used the fact that this type of function defines the angular spectrum of a 2D CFF, and generalized these ideas to the case of 3D classical wave fields, both scalar and vectorial. Our results show that all the angular spread measures used here provide values that are mutually similar when applied to the MUFs or the CFFs. By minimizing their rms difference, a one-to-one correspondence is established between the two classes of fields.

Of course, in addition to the results presented here, many possible generalizations along these lines emerges. These include the study of the higher-order eigenfunctions of the operator defining the MUFs and their connection to multipoles at complex locations, as well as the extension to the nonparaxial regime of fields emitted by partially coherent sources.

ACKNOWLEDGMENTS

M. A. Alonso acknowledges support from the start-up funds by The Institute of Optics, as well as Career Award PHY-0449708 by the National Science Foundation. He is also grateful for the hospitality and financial support during a visit to Università Roma Tre.

REFERENCES AND NOTES

1. M. Alonso, R. Borghi, and M. Santarsiero, “Nonparaxial fields with maximum joint spatial–directional localization. I. Scalar case,” *J. Opt. Soc. Am. A* **23**, 000–000 (2006).
2. M. Alonso, R. Borghi, and M. Santarsiero, “Nonparaxial fields with maximum joint spatial–directional localization. II. Vector case,” *J. Opt. Soc. Am. A* **23**, 000–000 (2006).
3. M. A. Alonso and G. W. Forbes, “Uncertainty products for nonparaxial wave fields,” *J. Opt. Soc. Am. A* **17**, 2391–2402 (2000).
4. Yu. A. Kravtsov, “Complex ray and complex caustics,” *Radiophys. Quantum Electron.* **10**, 719–730 (1967).
5. J. Arnaud, “Degenerate optical cavities. II: Effects of misalignments,” *Appl. Opt.* **8**, 1909–1917 (1969).
6. J. B. Keller and W. Streifer, “Complex rays with an application to Gaussian beams,” *J. Opt. Soc. Am.* **61**, 40–43 (1971).
7. G. A. Deschamps, “Gaussian beams as a bundle of complex rays,” *Electron. Lett.* **7**, 684–685 (1971).
8. L. B. Felsen, “Evanescence waves,” *J. Opt. Soc. Am.* **66**, 751–760 (1976).
9. S. Y. Shin and L. B. Felsen, “Gaussian beam modes by multipoles with complex source points,” *J. Opt. Soc. Am.* **67**, 699–700 (1977).
10. E. Heyman and L. B. Felsen, “Complex source pulse-beam fields,” *J. Opt. Soc. Am. A* **6**, 806–817 (1989).
11. E. Heyman and L. B. Felsen, “Gaussian beam and pulsed-beam dynamics: complex-source and complex-spectrum formulations within and beyond paraxial asymptotics,” *J. Opt. Soc. Am. A* **18**, 1588–1611 (2001).
12. C. J. R. Sheppard and S. Saghafi, “Beam modes beyond the paraxial approximation: a scalar treatment,” *Phys. Rev. A* **57**, 2971–2979 (1998).
13. C. J. R. Sheppard, “High-aperture beams,” *J. Opt. Soc. Am. A* **18**, 1579–1587 (2001).
14. A. L. Cullen and P. K. Yu, “Complex source-point theory of the electromagnetic open resonator,” *Proc. R. Soc. London, Ser. A* **366**, 155–171 (1979).
15. C. J. R. Sheppard and S. Saghafi, “Electromagnetic Gaussian beams beyond the paraxial approximation,” *J. Opt. Soc. Am. A* **16**, 1381–1386 (1999).
16. C. J. R. Sheppard and S. Saghafi, “Electric and magnetic dipole beams beyond the paraxial approximation,” *Optik* **110**, 487–491 (1999).
17. C. J. R. Sheppard and S. Saghafi, “Transverse-electric and transverse-magnetic beam modes beyond the paraxial approximation,” *Opt. Lett.* **24**, 1543–1545 (1999).
18. C. J. R. Sheppard, “Electromagnetic field in the focal region of wide-angular annular lens and mirror systems,” *IEE J. Microwaves, Opt. Acoust.* **2**, 163–166 (1978).
19. C. J. R. Sheppard and K. Larkin, “Optimal concentration of electromagnetic radiation,” *J. Mod. Opt.* **41**, 1495–1505 (1994).
20. P. Carruthers and M. M. Nieto, “Phase and angle variables in quantum mechanics,” *Rev. Mod. Phys.* **40**, 411–440 (1968).
21. T. Opatrný, “Mean value and uncertainty in optical phase—a simple mechanical analogy,” *J. Phys. A* **27**, 7201–7208 (1994).
22. T. Opatrný, “Number-phase uncertainty relations,” *J. Phys. A* **28**, 6961–6975 (1995).
23. It should be noted that the operator \mathcal{R}_s could be alternatively derived directly from Eq. (30) as

$$\mathcal{R}_s = (\mathbf{L} + iq\mathbf{e}_z \times \mathbf{u}) \cdot (\mathbf{L} - iq\mathbf{e}_z \times \mathbf{u}),$$

and on using the commutation relation given in Eq. (32).